RAPID COMMUNICATION | MARCH 08 2018

Communication: Modular path integral: Quantum dynamics via sequential necklace linking FREE

Nancy Makri

J. Chem. Phys. 148, 101101 (2018)
https://doi.org/10.1063/1.5024411
CHORUS

Communication: Modular path integral: Quantum dynamics via sequential necklace linking

Nancy Makri
Departments of Chemistry and Physics, University of Illinois, Urbana, Illinois 61801, USA

(Received 31 January 2018; accepted 22 February 2018; published online 8 March 2018)

It is shown that dynamical properties of extended systems (spin arrays, large organic molecules, or molecular aggregates) characterized primarily by local potential interactions (bond stretching, bending, and torsional interactions) can be obtained efficiently from fully quantum mechanical path integral calculations through sequential linking of the quantum paths or path integral necklaces corresponding to adjacent groups of atoms, which comprise the "modules." The scheme is applicable to complex chemical systems and is characterized by linear or sublinear scaling with system size. It is ideally suited to studies of vibrational energy flow and heat transport in long molecules (which may also be attached to solids), as well as simulations of exciton-vibration dynamics in molecular aggregates. *Published by AIP Publishing.* https://doi.org/10.1063/1.5024411

The wavefunction—the central object of quantum mechanics—requires storage which grows exponentially with the number of coupled degrees of freedom. This scaling impacts severely the feasibility of accurate numerical calculations, restricting them to systems of only a few particles. Overcoming this exponential scaling without introducing approximations appears feasible either if some factorization is possible or by resorting to wavefunction-free procedures. Perhaps the most widely used approach in this latter category is the path integral Monte Carlo (PIMC) method[1–3] (along with its molecular dynamics variant[4]), which is based on Feynman's path integral[5,6] representation of quantum statistical mechanics.[7] PIMC calculations of thermal equilibrium properties are numerically exact (i.e., converge to the full quantum mechanical result) and (for spinless or boson particles) rather efficient, requiring computational effort that scales weakly with the number of particles. Unfortunately, extension of these methods to real-time properties is impractical because of the "sign problem," i.e., the inability of Monte Carlo methods[8] to account in an efficient manner for the dramatic phase cancellation that results from the oscillatory real-time propagator.

Because of particle correlation, full factorization of a many-body wavefunction (or its generalization, the density matrix) is not possible in general, except as a mean-field approximation. On the other hand, tensor decompositions often provide efficient and accurate tools for studying correlated systems. In particular, the density matrix renormalization group[9] (DMRG) approach allows in some cases accurate calculations with efficient scaling. DMRG methods are ideally suited to ground state calculations of extended one-dimensional systems, although finite-temperature[10] and time-dependent[11] variants are also available. Furthermore, tensor decompositions (in time) of the real-time path integral[12–15] lead to iterative evaluation, allowing numerically exact calculations of dynamical processes in quantum dissipative systems with cost that grows linearly with propagation time.

The present communication introduces a tensor decomposition of the path integral, which enables accurate and efficient calculations of dynamical properties in extended (not necessarily periodic) systems characterized by some degree of locality, i.e., where potential interactions of each particle are limited to a small number of neighboring particles. Rather than propagating a spatial representation of the many-particle density matrix, which requires storage that scales exponentially with the number of particles, the proposed modular path integral (MPI) algorithm sums discretized quantum paths with respect to each "module" (site, atom, or group of directly correlated particles) by linking the path integral necklaces sequentially and leads to linear scaling with system size.

The efficiency of the proposed MPI approach depends on one's ability to store the discretized Feynman paths for a single particle or module, and one can easily envision situations where the proposed scheme will not be practical. Still, there are many systems with intriguing dynamical effects, where the module consists of a small number of degrees of freedom and where time discretization of the path integral is possible with only a modest number (e.g., 10-20) of time steps. For example, chains of interacting spins, which serve as important models for quantum phase transitions, are ideally suited to this approach. Studies of intramolecular energy transfer in long molecules (such as hydrocarbon chains), which can be adequately described in terms of spectroscopically determined force fields with local potential interactions, should also be feasible with this approach. The current understanding of heat flow in such systems is limited because anharmonic interactions are important, while classical trajectory studies are unable to account properly for zero-point energy. Exciton transport in arrays of molecular aggregates should also be amenable to the MPI methodology. It should be emphasized that the MPI algorithm does not rely on periodicity or even a simple composition of the system under study but is easily applicable to complex molecules with branched backbones or rings, as long as potential interactions are relatively local.

To illustrate the idea, consider first a one-dimensional chain of n atoms (of masses $m^{(i)}$), whose Cartesian coordinates are labeled $x^{(1)}, x^{(2)}, \ldots, x^{(n)}$ and denoted collectively by the n-component vector $\mathbf{x}$. In this simple model, it is assumed that each atom experiences the potential $u(x^{(i)})$ and interacts with its nearest neighbors through the (anharmonic) potential $V_{i,i+1}(x^{(i)}, x^{(i+1)})$. The total Hamiltonian is thus given by the expression

$$\hat{H} = -\sum_{i=1}^{n} \frac{\hbar^2}{2m^{(i)}} \frac{\partial^2}{\partial x^{(i)2}} + \sum_{i=1}^{n} u_i(\hat{x}^{(i)}) + \sum_{i=1}^{n-1} V_{i,i+1}(\hat{x}^{(i)}, \hat{x}^{(i+1)}). \tag{1}$$

Dynamical properties of interest can be obtained from the time evolution of observables or through time correlation functions. Consider the symmetrized, complex time correlation function of the operators $\hat{A}$ and $\hat{B}$, which correspond to the properties of atoms α and β, respectively, and

$$C_{\alpha\beta}(t) = Z^{-1}\mathrm{Tr}\left(e^{i\hat{H}t_c^*/\hbar}\,\hat{A}_\alpha\, e^{-i\hat{H}t_c/\hbar}\hat{B}_\beta\right), \tag{2}$$

where Z is the quantum partition function and the complex time is $t_c = t - i\hbar\beta/2$ (where t is the propagation time and $\beta = 1/k_B T$ is the inverse temperature). For simplicity, it is assumed here that the operators are functions of the coordinates of these atoms. (Momentum-dependent operators are easily accounted for within the Trotter factorization[16] of the propagators, leading to a minor modification of the integrand which does not change the structure of the MPI scheme. Likewise, it is obvious that operators which depend on the coordinates of adjacent atoms, e.g., properties pertaining to bond lengths, can also be treated straightforwardly, without a significant modification of the algorithm.) The complex-time correlation function offers some computational advantages because the pairing of the real time evolution operator with the Boltzmann operator helps reduce the oscillatory character of the former. Flux correlation functions,[17] which yield reaction and transport rates, are most conveniently expressed in this form. The complex- and real-time correlation functions are connected by a simple relation in Fourier space.[18]

To proceed, the trace is evaluated in the coordinate representation and the complex time evolution operators are discretized into time steps of length $\Delta t_c = t_c/N$, where N is an integer, resulting in the following expression for the correlation function:

$$\begin{aligned} C_{\alpha\beta}(t) = \int d\mathbf{x}_1 \int d\mathbf{x}_2 \cdots \int d\mathbf{x}_{2N} B(\mathbf{x}_{2N}) \langle \mathbf{x}_{2N}| \\ \times e^{i\hat{H}\Delta t_c^*/\hbar} |\mathbf{x}_{2N-1}\rangle \cdots \langle \mathbf{x}_{N+1}|\, e^{i\hat{H}\Delta t_c^*/\hbar} |\mathbf{x}_N\rangle A(\mathbf{x}_N) \\ \times \langle \mathbf{x}_N|\, e^{-i\hat{H}\Delta t_c/\hbar} |\mathbf{x}_{N-1}\rangle \cdots \langle \mathbf{x}_1|\, e^{-i\hat{H}\Delta t_c/\hbar} |\mathbf{x}_{2N}\rangle . \end{aligned} \tag{3}$$

Use of the Trotter factorization[16] of the short-time evolution operators brings the correlation function to the form

$$\begin{aligned} C_{\alpha\beta}(t) = \int dx_1^{(1)} \cdots dx_{2N}^{(1)} \cdots \int dx_1^{(n)} \cdots dx_{2N}^{(n)} e^{-\frac{i}{\hbar}\sum_{k=N+1}^{2N}\sum_{i=1}^{n}\frac{m^{(i)}}{2\Delta t_c^*}\left(x_k^{(i)}-x_{k-1}^{(i)}\right)^2 + \frac{i}{\hbar}\Delta t_c^* \sum_{k=N}^{2N}\eta_k\left(\sum_{i=1}^{n} u_i(x_k^{(i)}) + \sum_{i=1}^{n-1} V_{i,i+1}(x_k^{(i)}, x_k^{(i+1)})\right)} \\ \times e^{\frac{i}{\hbar}\sum_{k=1}^{N}\sum_{i=1}^{n}\frac{m^{(i)}}{2\Delta t_c}\left(x_k^{(i)}-x_{k-1}^{(i)}\right)^2 - \frac{i}{\hbar}\Delta t_c \sum_{k=0}^{N}\eta_k\left(\sum_{i=1}^{n} u_i(x_k^{(i)}) + \sum_{i=1}^{n-1} V_{i,i+1}(x_k^{(i)}, x_k^{(i+1)})\right)} B(x_{2N}^{(\beta)}) A(x_N^{(\alpha)}), \end{aligned} \tag{4}$$

where $\eta_k = \frac{1}{2}$ if $k = 0, N$, or $2N$ and $\eta_k = 1$ otherwise, and $x_0^{(i)} = x_{2N}^{(i)}$. In the context of the equilibrium ($t = 0$) path integral, the auxiliary variables $x_1^{(i)}, \ldots, x_{2N}^{(i)}$ are referred to as "beads" and the quantum thermodynamics of each atom is isomorphic to the classical configuration integral for the $2N$-bead "necklace."[19] In the general case of nonzero real time, the concept of the necklace remains valid although the exponent is now complex-valued and no longer describes a classical equilibrium quantity.

Examination of Eq. (4) reveals two types of interactions among beads. First, as usual, each bead is coupled to the two neighboring beads of the same atom via the kinetic energy terms in the path integral expression. Second, each bead of an atom is coupled via potential terms to the corresponding bead of the necklaces representing the two adjacent atoms. This is a consequence of the locality of interactions in the chain model. The above observations imply that the path integral variables are connected on a cylindrical lattice, as illustrated in Fig. 1.

For a long chain ($n \gg 10$), the Hilbert space is very large, prohibiting storage of a wavefunction or density matrix on a spatial grid for subsequent iterative propagation in time. However, the thermodynamic properties of atoms are adequately quantized with a relatively small number of beads at room temperature. Furthermore, correlation functions in molecular systems often decay within a time of order $\hbar\beta$.[20] This implies that the number of beads required to converge

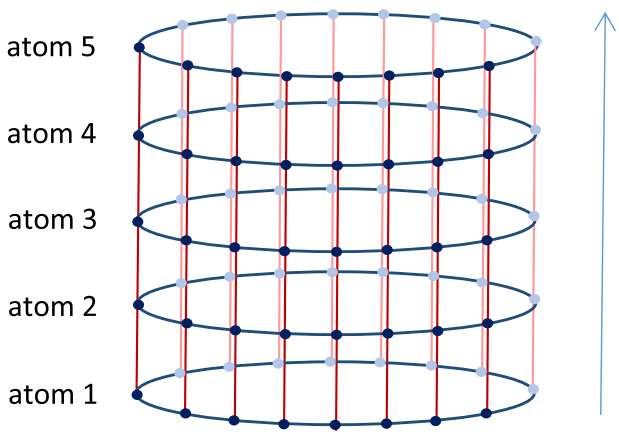

FIG. 1. Schematic illustration of bead connections. Dark and light blue circles correspond to beads 1, . . ., N and N + 1, . . ., 2N, respectively. Blue links describe kinetic energy couplings. Red lines correspond to potential interactions.

the complex-time correlation function typically is not very large, i.e., $2N \sim 10$–$20 \ll n$. The simple connectivity of the path integral variables suggests the evaluation of the correlation function via an iterative procedure along the molecular backbone (the vertical direction in Fig. 1), i.e., by integrating the path integral necklaces atom by atom according to the relation

$$R^{(i+1)}\left(x_1^{(i+1)},\ldots,x_{2N}^{(i+1)}\right) = \int dx_1^{(i)}\cdots\int dx_{2N}^{(i)}\, T^{(i)}\left(x_1^{(i+1)},\ldots,x_{2N}^{(i+1)};x_1^{(i)},\ldots,x_{2N}^{(i)}\right) \times R^{(i)}\left(x_1^{(i)},\ldots,x_{2N}^{(i)}\right)\gamma_i, \quad i=1,\ldots,n-1, \tag{5}$$

where $\mathbf{R}^{(i)}$ holds the result of the necklace propagation through atom i, $\mathbf{T}^{(i)}$ is the propagator matrix which connects atoms i and $i+1$, given by

$$T^{(i)}\left(x_1^{(i+1)},\ldots,x_{2N}^{(i+1)};x_1^{(i)},\ldots,x_{2N}^{(i)}\right) = e^{-\frac{i}{\hbar}\sum_{k=N+1}^{2N}\frac{m^{(i+1)}}{2\Delta t_c^*}\left(x_k^{(i+1)}-x_{k-1}^{(i+1)}\right)^2+\frac{i}{\hbar}\Delta t_c^*\sum_{k=N}^{2N}\eta_k\left(u_{i+1}(x_k^{(i+1)})+V_{i,i+1}(x_k^{(i)},x_k^{(i+1)})\right)} \times e^{\frac{i}{\hbar}\sum_{k=1}^{N}\frac{m^{(i+1)}}{2\Delta t_c}\left(x_k^{(i+1)}-x_{k-1}^{(i+1)}\right)^2-\frac{i}{\hbar}\Delta t_c\sum_{k=0}^{N}\eta_k\left(u_{i+1}(x_k^{(i+1)})+V_{i,i+1}(x_k^{(i)},x_k^{(i+1)})\right)} \tag{6}$$

and

$$\gamma_i = \begin{cases} A(x_N^{(\alpha)}), & i=\alpha,\\ B(x_{2N}^{(\beta)}), & i=\beta,\\ 1, & i\neq\alpha,\beta. \end{cases} \tag{7}$$

The procedure is initialized with the array $\mathbf{R}^{(1)}$ whose elements are given by

$$R^{(1)}\left(x_1^{(1)},\ldots,x_{2N}^{(1)}\right) = e^{-\frac{i}{\hbar}\sum_{k=N+1}^{2N}\frac{m^{(1)}}{2\Delta t_c^*}\left(x_k^{(1)}-x_{k-1}^{(1)}\right)^2+\frac{i}{\hbar}\Delta t_c^*\sum_{k=N}^{2N}\eta_k u_1(x_k^{(1)})+\frac{i}{\hbar}\sum_{k=1}^{N}\frac{m^{(1)}}{2\Delta t_c}\left(x_k^{(1)}-x_{k-1}^{(1)}\right)^2-\frac{i}{\hbar}\Delta t_c\sum_{k=0}^{N}\eta_k u_1(x_k^{(1)})}. \tag{8}$$

For simplicity, Eqs. (3)–(8) were given for the case where all atoms are quantized by the same number N of beads. However, it should be clear that the path integral expression and its sequential evaluation described above can be easily adapted to the use of different numbers of beads for different atoms, which can be chosen based on atomic masses and the desired degree of quantization.

Since the number of necklace configurations equals M^{2N}, where M is the number of grid points required to represent each atom, storage of all possible necklace configurations is impractical. Discrete variable representations of the path integral[21] may be employed to produce compact grids for each atom. The exponentially decaying component of the complex-time propagator ensures that the vast majority of bead arrangements lead to negligible weights, allowing Monte Carlo selection of the statistically important necklace configurations for inclusion in the array $\mathbf{R}$. The selected necklace configurations of each atom can be thought of as grid points, and the propagation shown in Eq. (5) is a matrix-vector multiplication that is repeated along the molecular chain. Thus, the scheme resembles the iterative (in time) Monte Carlo (IMC) methodology,[22–24] with the important difference that the present MPI algorithm involves iteration in particle space, rather than time. As discussed earlier, Monte Carlo methods cannot handle efficiently the oscillatory character of the real- or complex-time path integral, Eq. (4). However, Eq. (5) involves integration in a small subspace (in this present example, the bead coordinates of a single atom), and thus, the sign problem will be considerably less severe. This behavior was clearly illustrated through IMC calculations in multidimensional systems.[24] Convergence may be further enhanced by implementing some of the techniques discussed below in the context of real-time correlation functions.

The real-time implementation of the scheme described above amounts to a minor modification of the MPI structure, replacing the complex time necklaces by forward-backward paths linked together by an imaginary time segment. Of major concern in this context might be the highly oscillatory character of the Trotter real-time propagator and the lack of compact support (i.e., absence of a spatially confining function) in the real-time portion of Eq. (4), which would prohibit the use of Monte Carlo. However, energy filtering of the propagator[25,26] and/or the use of discrete variable representations of the path integral[21] eliminate the rapid oscillations and allow weight-based selection. Furthermore, there are deterministic alternatives to the Monte Carlo selection of necklace configurations. In addition to the use of weight-based path construction criteria,[27,28] recent work on the real-time path integral for quantum dissipative systems has shown that blip regions are associated with damping.[29,30] This observation stems from the decoherence-inducing nature of general many-particle environments[31] and should provide a powerful selection criterion for the implementation of the MPI idea on real-time correlation functions or for propagating the density matrix.

The MPI methodology is illustrated below with a model chain or two-level systems (TLS) connected through Ising-type (nearest neighbor) interactions. The Hamiltonian is given by the expression

$$\hat{H} = -\hbar\Omega\sum_{i=1}^{n}\hat{\sigma}_x^{(i)} + u\sum_{i=1}^{n-1}\hat{\sigma}_z^{(i)}\hat{\sigma}_z^{(i+1)}, \tag{9}$$

where $\hat{\sigma}_x$, $\hat{\sigma}_z$ are the Pauli spin operators, $2\hbar\Omega$ is the common tunneling splitting, and u is the spin-spin coupling strength. Figure 2 shows the obtained complex-time autocorrelation function of a spin position (i.e., $\hat{A} = \hat{B} = \hat{\sigma}_z^{(\alpha)}$) of the first ($\alpha = 1$), second ($\alpha = 2$), and middle ($\alpha = 25$) spin in a chain of $n = 50$ connected spins at the intermediate temperature $\hbar\Omega\beta = 1$. The complex time discretization converged with

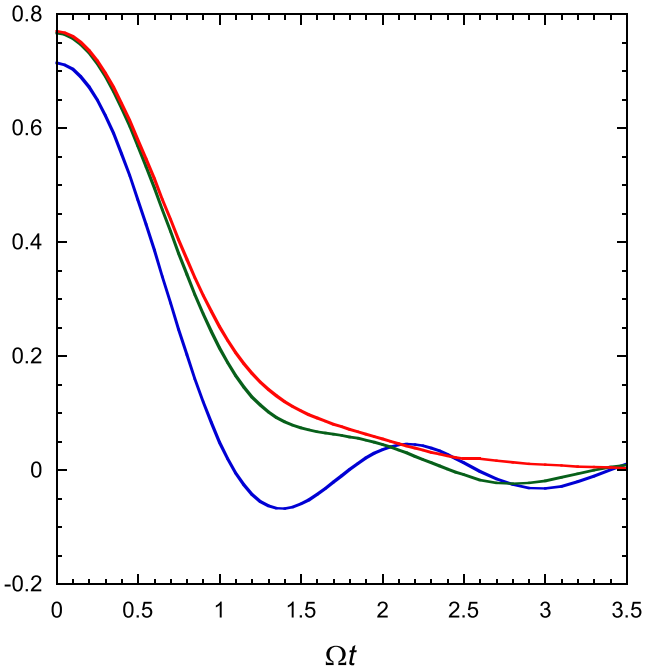

FIG. 2. Complex-time autocorrelation function of $\hat{\sigma}_z$ for a spin in a chain of 50 coupled spins with the parameters given in the text. Blue line: correlation function of spin 1. Green line: correlation function of spin 2. Red line: correlation function of spin 25.

up to $2N = 16$ beads; thus, no weight-based necklace selection was necessary. The figure shows that the edge spin, which is linked to the rest of the chain only on one side, maintains a substantial degree of coherence with these parameters. Coherence is significantly quenched for the second spin, while the spin at the center of the long chain displays incoherent decay.

The basic MPI scheme described above may be extended to investigate the intramolecular vibrational dynamics of a long molecule. Consider a long hydrocarbon with single and multiple bonds. Accurate, spectroscopically determined molecular force fields are available in internal coordinates, which give the potential energy as a function of bond lengths and bending and dihedral angles.[32,33] In order to account for these interactions, the basic propagation module must be augmented such that all atoms that are coupled directly are contained in adjacent modules. The size of (number of atoms contained in) each module depends on the topology of the atom-atom interactions. For example, the basic module in a linear hydrocarbon chain consists of two carbon atoms if one wishes to account explicitly only for bond stretches and bends. The basic modules and the sequence of necklace linking for such a system are illustrated in Fig. 3. Treating torsional interactions explicitly (in addition to bond stretching and bending terms) involves a basic module of three carbon atoms. Bonded hydrogen atoms would also be included with the carbon atoms of each module and could be kept rigidly bonded or treated explicitly.

Chain branching requires an augmented module at the linked site, as illustrated in Fig. 3. Starting from the end of the main chain, one proceeds to sequentially link modules along the main molecular backbone. Once the module adjacent to that containing the branching site is reached, the propagation pauses and one begins to link the modules of the side chain,

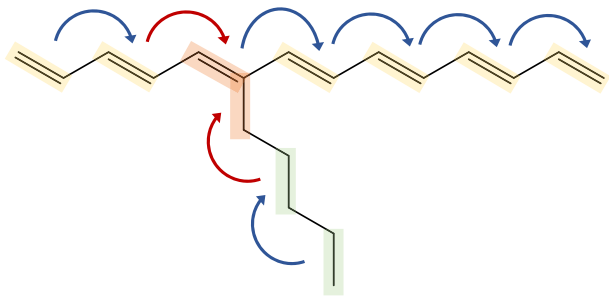

FIG. 3. A segment of a branched hydrocarbon chain, illustrating the carbon atoms included in each module and the sequence of module linking. It is assumed that only bond stretching and bending interactions are included. Each color shading indicates a particular module type. The blue arrows represent sequential linking, while the red arrows represent simultaneous linking.

starting again from the end and proceeding toward the branching site. Then both treated chains are linked to the branching site module and the linking continues in the direction of the molecular backbone until another side chain is encountered. The MPI procedure can easily be extended to treat cyclic groups and (at somewhat higher computational cost) one or two distant interactions, such as those arising from polar groups.

Note that identical modules require precisely the same treatment, eliminating a large number of operations for a long molecule. Thus, the MPI scheme proceeds by combining elementary modules to form larger molecular segments (side chains, rings, or backbone segments) which are eventually joined to complete the propagation. While such segments may repeat several times in a large molecule, the calculations required for each fragment need to be performed just once. The methodology can easily be augmented with the addition of heat baths mimicking the interaction of one or both ends of a molecular chain with solids.

The MPI scheme described in this communication is fully quantum mechanical and involves no *ad hoc* assumptions. It allows the treatment of potential interactions in large systems with chemical complexity (as long as the majority of such interactions are sufficiently local) and scales linearly or better (as identical segments need be treated only once) with system size. It is expected that MPI calculations will shed light on the intricate interplay among potential anharmonicity, zero-point energy, and quantum interference effects on the intramolecular dynamics and heat flow along realistic molecular systems which may be isolated, attached to solids,[34] or serve as molecular junctions, complementing studies on small molecular systems[35–37] or idealized models.[38–40]

Finally, by combining the treatment of intramolecular vibrations within individual monomers with inter-monomer electronic coupling, the MPI approach should offer an efficient and highly accurate approach to the treatment of charge transfer and exciton-vibration dynamics in molecular aggregates that hold promise for solar energy harvest and storage.

This material is based upon work supported by the National Science Foundation under Award No. CHE-1665281.

[1]L. D. Fosdick and H. F. Jordan, Phys. Rev. **143**, 58–66 (1966).
[2]S. V. Lawande, C. A. Jensen, and H. L. Sahlin, J. Comput. Phys. **3**, 416–443 (1969).

[3]B. Bernu and D. M. Ceperley, in *Quantum Simulations of Complex Many-Body Systems: From Theory to Algorithms*, edited by J. Grotendorst, D. Marx, and A. Muramatsu (John von Neumann Institute for Computing, 2002), Vol. 10.
[4]M. Parrinello and A. Rahman, J. Chem. Phys. **80**, 860–867 (1984).
[5]R. P. Feynman, Rev. Mod. Phys. **20**, 367–387 (1948).
[6]R. P. Feynman and A. R. Hibbs, *Quantum Mechanics and Path Integrals* (McGraw-Hill, New York, 1965).
[7]R. P. Feynman, *Statistical Mechanics* (Addison-Wesley, Redwood City, 1972).
[8]N. Metropolis, A. W. Rosenbluth, M. N. Rosenbluth, H. Teller, and E. Teller, J. Chem. Phys. **21**, 1087–1092 (1953).
[9]S. R. White, Phys. Rev. Lett. **69**, 2863 (1992).
[10]A. E. Feiguin and S. R. White, Phys. Rev. B **72**, 220401 (2005).
[11]S. R. White and A. E. Feiguin, Phys. Rev. Lett. **93**, 076401 (2004).
[12]D. E. Makarov and N. Makri, Chem. Phys. Lett. **221**, 482–491 (1994).
[13]N. Makri and D. E. Makarov, J. Chem. Phys. **102**, 4600–4610 (1995).
[14]N. Makri and D. E. Makarov, J. Chem. Phys. **102**, 4611–4618 (1995).
[15]N. Makri, J. Chem. Phys. **111**, 6164–6167 (1999).
[16]M. F. Trotter, Proc. Am. Math. Soc. **10**, 545–551 (1959).
[17]W. H. Miller, S. D. Schwartz, and J. W. Tromp, J. Chem. Phys. **79**, 4889–4898 (1983).
[18]R. Kubo, M. Toda, and N. Hashitsume, *Statistical Physics*, 2nd ed. (Springer-Verlag, Heidelberg, 1991).
[19]D. Chandler and P. G. Wolynes, J. Chem. Phys. **74**, 4078–4095 (1981).
[20]J. W. Tromp and W. H. Miller, J. Phys. Chem. **90**, 3482–3485 (1986).
[21]M. Topaler and N. Makri, Chem. Phys. Lett. **210**, 448 (1993).
[22]V. Jadhao and N. Makri, J. Chem. Phys. **129**, 161102 (2008).
[23]V. Jadhao and N. Makri, J. Chem. Phys. **132**, 104110 (2010).
[24]V. Jadhao and N. Makri, J. Chem. Phys. **133**, 114105 (2010).
[25]N. Makri, Chem. Phys. Lett. **159**, 489–498 (1989).
[26]N. Makri, J. Phys. Chem. **97**, 2417–2424 (1993).
[27]E. Sim, J. Chem. Phys. **115**, 4450–4456 (2001).
[28]R. Lambert and N. Makri, Mol. Phys. **110**, 1967–1975 (2012).
[29]N. Makri, J. Chem. Phys. **141**, 134117 (2014).
[30]N. Makri, Chem. Phys. Lett. **593**, 93–103 (2014).
[31]N. Makri, Faraday Discuss. **195**, 81–92 (2016).
[32]K. Palmö, N. G. Mirkin, L.-O. Pietilä, and S. Krimm, Macromolecules **26**, 6831–6840 (1993).
[33]C. S. Ewig, R. Berry, U. Dinur, J.-R. Hill, M.-J. Hwang, H. Li, C. Liang, J. Maple, Z. Peng, T. P. Stockfisch, T. S. Thacher, L. Yan, X. Ni, and A. T. Hagler, J. Comput. Chem. **22**, 1782–1800 (2001).
[34]Z. Wang, J. A. Carter, A. Lagutchev, Y. K. Koh, N.-H. Seong, D. G. Cahill, and D. D. Dlott, Science **317**, 787–790 (2007).
[35]A. T. Maynard and R. E. Wyatt, J. Chem. Phys. **103**, 8372 (1995).
[36]R. Bigwood, M. Gruebele, D. M. Leitner, and P. G. Wolynes, Proc. Natl. Acad. Sci. U. S. A. **95**, 5960–5964 (1998).
[37]D. Shemesh and R. B. Gerber, J. Phys. Chem. A **110**, 8401–8408 (2006).
[38]U. Zurcher and P. Talkner, Phys. Rev. A **42**, 3278–3290 (1990).
[39]D. Segal and A. Nitzan, J. Chem. Phys. **119**, 6840–6855 (2003).
[40]D. Segal and B. K. Agarwalla, Annu. Rev. Phys. Chem. **67**, 185–209 (2016).